



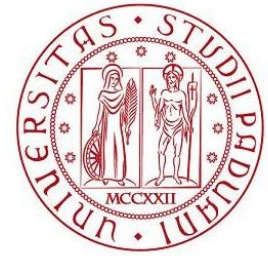
Discontinuous mechanical problems studied with a Peridynamics-based approach

Provided by: Soheil Bazazzadeh

Supervisor: Prof Ugo Galvanetto

Advisor: Prof Mirco Zaccariotto

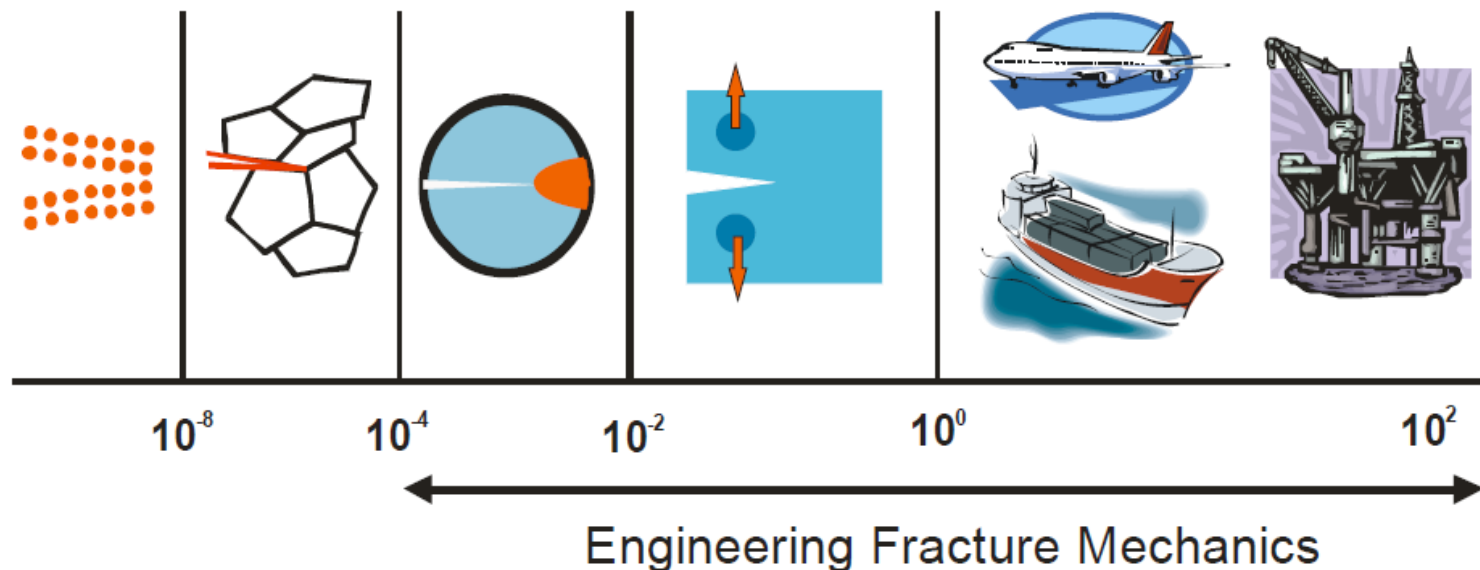
Index



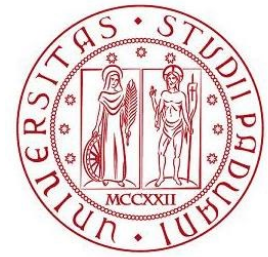
-
- ❑ Introduction to discontinuous problems
 - ❑ Introduction to Peridynamics
 - ❑ Fatigue crack growth
 - Aspects of modelling fatigue crack propagation
 - Description of cylindric model
 - Description of bilinear constitutive laws and three fatigue degradation strategies
 - Numerical Results
 - Peridynamics implementation of the fatigue model
 - ❑ Simulation of thermo-mechanical problems in brittle materials using an adaptive multi-grid peridynamic method
 - Introduction to Thermo-mechanical problems
 - Coupling of grids with different spacing
 - Crack propagation with adaptivity
 - Thermal shock examples
 - ❑ Simulation of 2D/3D sloshing phenomena by using the Peridynamic differential operator
 - Introduction to sloshing problems
 - The Peridynamic differential operator numerical solution (PDDO)
 - Solving fluid equations with moving boundaries using PDDO
 - Sloshing problems
 - ❑ Conclusions

Discontinuous problems

- The classical continuum theory of solid mechanics **basically employs partial derivatives in the equation of motion** and accordingly requires the differentiability of the displacement field. Such an assumption breaks down when simulation of problems containing **discontinuities, such as cracks**, comes into the picture.

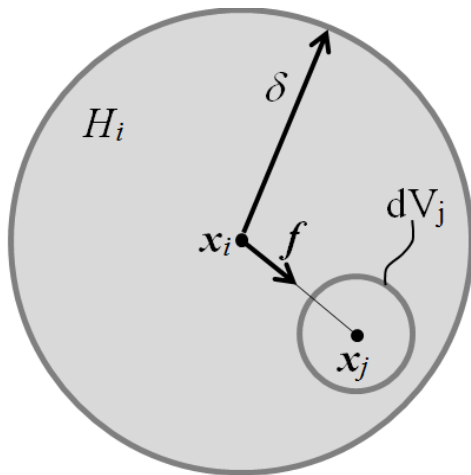


Fundamentals of peridynamics



- The equation of motion is defined by means of an integral operator as:

$$\rho \ddot{\mathbf{u}}(\mathbf{x}_i, t) = \int_{H_{xi}} \mathbf{f}(\mathbf{u}(\mathbf{x}_j, t) - \mathbf{u}(\mathbf{x}_i, t), \mathbf{x}_j - \mathbf{x}_i) dV_j + \mathbf{b}(\mathbf{x}_i, t) \quad \forall \mathbf{x}_j \in H_{xi}$$



- The **Pairwise Force Function** expresses the vector force of the interaction (called *bond*) between \mathbf{x}_i and \mathbf{x}_j

$$\mathbf{f}(\boldsymbol{\eta}, \boldsymbol{\xi}) = f(y, \xi, t) \frac{\boldsymbol{\xi} + \boldsymbol{\eta}}{\|\boldsymbol{\xi} + \boldsymbol{\eta}\|}$$

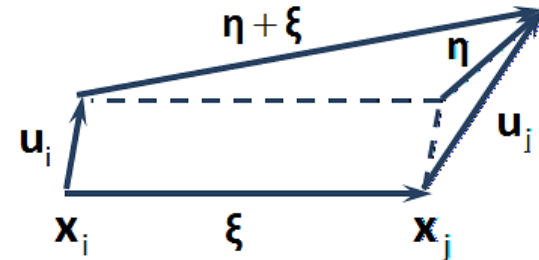
$\mathbf{u} \rightarrow$ displacement vector field

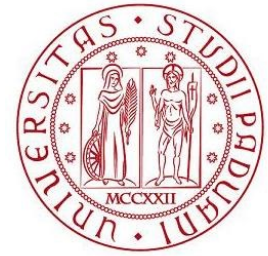
$\rho \rightarrow$ mass density

$\mathbf{b} \rightarrow$ body force density

$\boldsymbol{\xi} = \mathbf{x}_j - \mathbf{x}_i \rightarrow$ initial relative position

$\boldsymbol{\eta} = \mathbf{u}_j - \mathbf{u}_i \rightarrow$ relative displacement





Fundamentals of peridynamics

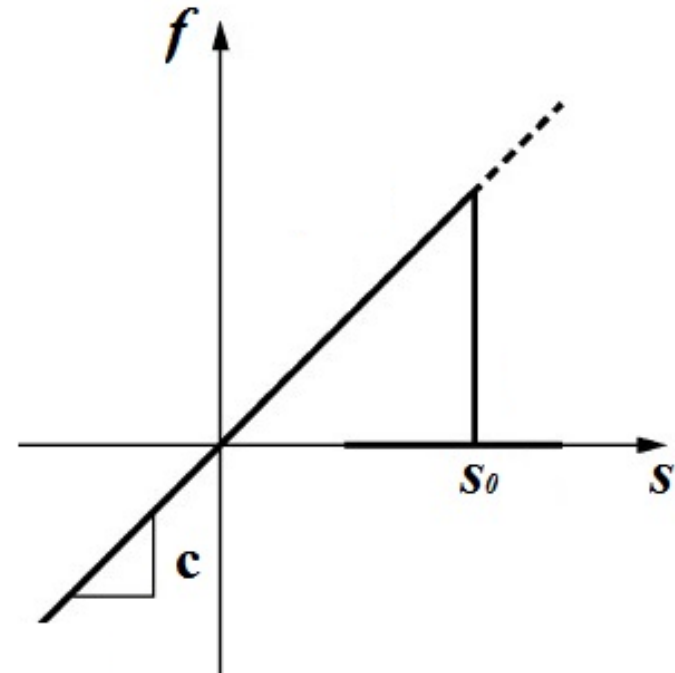
- The PairWise force function is defined, for a linear elastic material, by means of the following expression (on plane behavior):

$$f(\boldsymbol{\eta}, \boldsymbol{\xi}) = c \cdot s \frac{\boldsymbol{\xi} + \boldsymbol{\eta}}{\|\boldsymbol{\xi} + \boldsymbol{\eta}\|}$$

$$c \propto \frac{E}{\delta^3} \rightarrow \text{bond stiffness}$$

$$s = \frac{\|\boldsymbol{\xi} + \boldsymbol{\eta}\| - \|\boldsymbol{\xi}\|}{\|\boldsymbol{\xi}\|} \rightarrow \text{bond stretch}$$

$$s_0 \propto \sqrt{G_0/E\delta} \rightarrow \text{critical bond stretch}$$

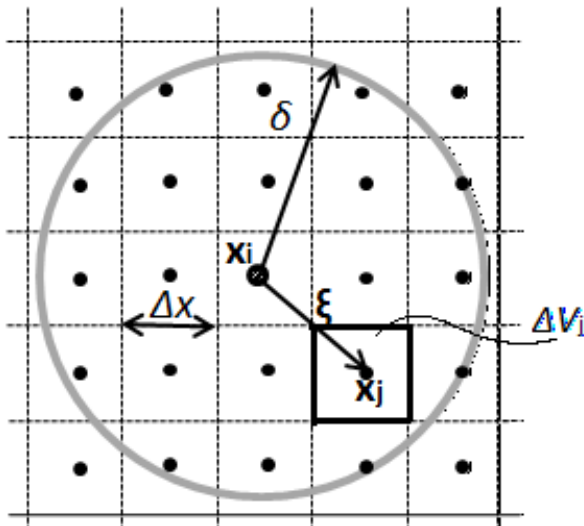


$E \rightarrow$ Young's modulus

$G_0 \rightarrow$ Fracture energy in mode I

Numerical discretization

In the numerical implementation of the peridynamic approach, the body is discretized into grid points called **nodes**.



Discretization:

Dynamic analysis formulation

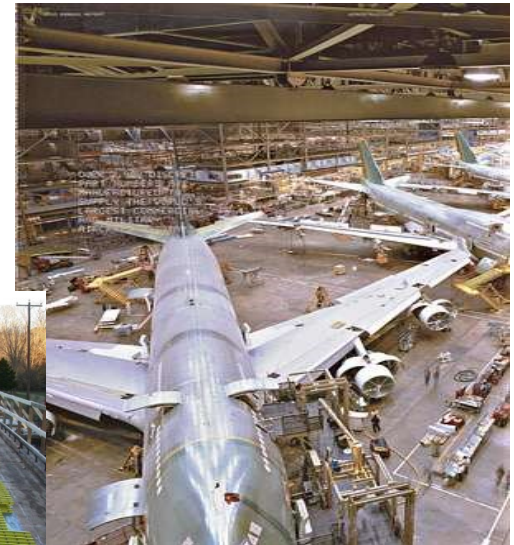
$$\rho \ddot{\mathbf{u}}_i^n = \sum_j \mathbf{f}(\mathbf{u}_j^n - \mathbf{u}_i^n, \mathbf{x}_j - \mathbf{x}_i) \Delta V_j + \mathbf{b}_i^n \quad \text{Explicit solver}$$

Static analysis formulation

$$0 = \sum_j \mathbf{f}(\mathbf{u}_j^n - \mathbf{u}_i^n, \mathbf{x}_j - \mathbf{x}_i) \Delta V_j + \mathbf{b}_i^n \quad \text{Implicit solver}$$

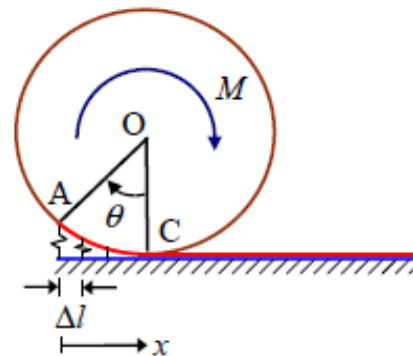
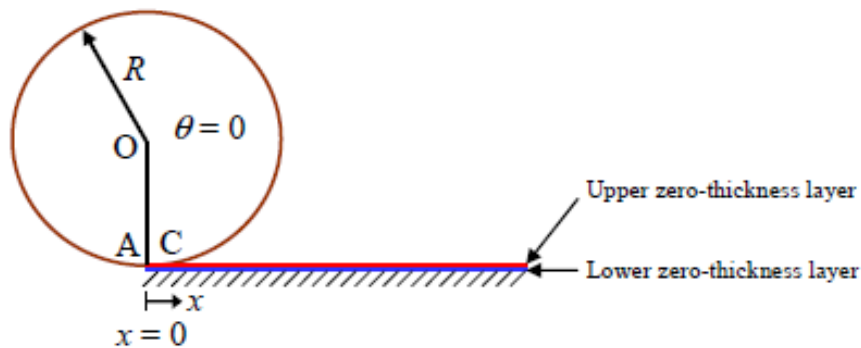
Damage under high cycle fatigue

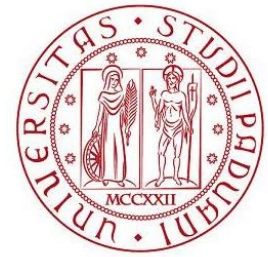
- Light weight structures with high resistance and stiffness
- Ocean, Maritime in coastal engineering
- Aerospace engineering
- Industrial engineering and transportation industry



Cylinder model

- Consider a cylinder of radius R which, under static loading, rolls in a clockwise direction on a horizontal surface.
- The lower layer is fixed. The upper layer adheres to the surface of the cylinder at the contact point, C and remains adhered.
- As the cylinder rotates and the contact point advances as the cylinder rolls along the horizontal surface the angle swept through by OA is the rotation, θ , of the cylinder.





In fatigue problems two components of damage are considered

1-Static damage $\longrightarrow D_s$

2-Fatigue damage $\longrightarrow D_f$

Stiffness degradation damage

In this approach the total damage, D , can be considered a measure of the degradation of the initial stiffness

$$\sigma = (1 - D) K \delta$$



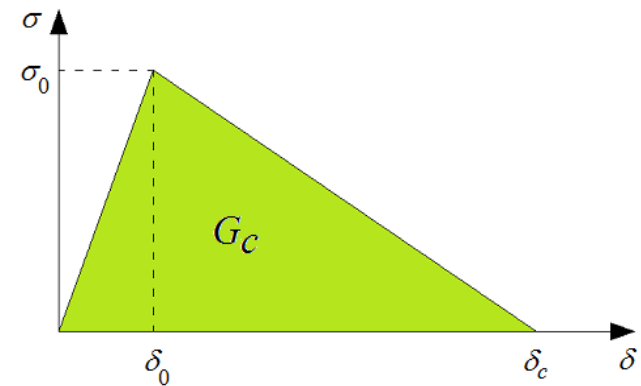
$$D_s + D_f$$

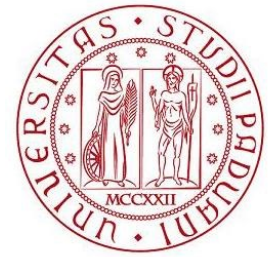
$\delta \longrightarrow$ Elongation in a spring

D_s can be written as

$$D_s = \begin{cases} 0 & 0 \leq \delta \leq \delta_0 \\ \left(\frac{\delta - \delta_0}{\delta} \right) \left(\frac{\delta_c}{\delta_c - \delta_0} \right) & \delta_0 < \delta < \delta_c \\ 1 & \delta \geq \delta_c \end{cases}$$

K is the stiffness: $K = \sigma_0 / \delta_0$





Static and Fatigue degradation strategies

□ Rate of change of the static damage


$$\frac{\partial D_s}{\partial t} = \frac{\delta_0 \delta_c}{\delta_c - \delta_0} \frac{\dot{\delta}}{\delta^2} \quad \delta_0 < \delta < \delta_c$$

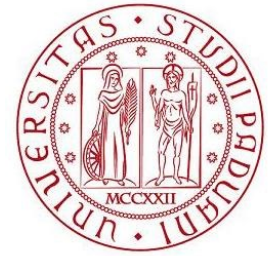
$$D_{sN+\Delta N} - D_{sN} = \frac{\delta_0 \delta_c}{\delta_c - \delta_0} \left(\frac{1}{\delta_N} - \frac{1}{\delta_{N+\Delta N}} \right)$$

□ **Fatigue** damage Strategies

First strategy

Second strategy

Third strategy



First strategy

Fatigue rate is

$$\dot{D} = Ce^{\lambda D} \left(\frac{\delta}{\delta_c} \right)^\beta$$

Increment of fatigue damage



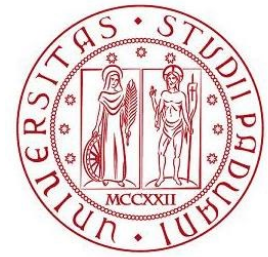
$$D_{fN+\Delta N} - D_{fN} = \Delta N \frac{C}{1+\beta} e^{\lambda D_\mu} \left(\frac{\delta_\mu}{\delta_c} \right)^{1+\beta}$$

The increment of total damage due to an increment of the number of cycles (ΔN) is

$$D_{N+\Delta N} - D_N = \underbrace{\frac{\delta_0 \delta_c}{\delta} \left(\frac{1}{\delta} - \frac{1}{\delta_c} \right)}_{\text{sum}} + \underbrace{\Delta N \frac{C}{1+\beta} e^{\lambda D_\mu} \left(\frac{\delta_\mu}{\delta_c} \right)^{1+\beta}}_{\text{average}}$$

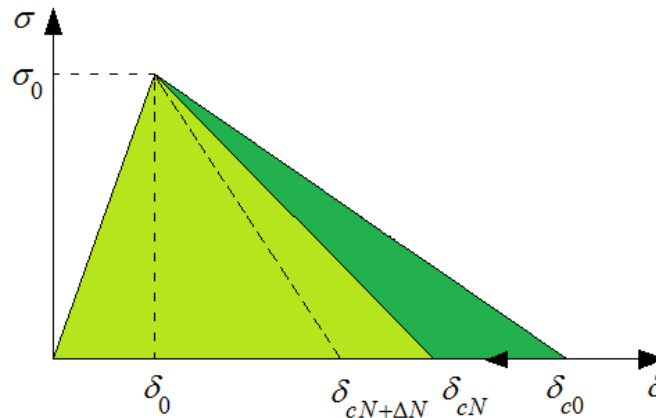
$$D_\mu = (1-\mu)D_N + \mu D_{N+\Delta N}$$

$$\delta_\mu = (1-\mu)\delta_N + \mu\delta_{N+\Delta N}$$



Second strategy

Failure elongation of a spring in each increment of load cycle, ΔN , is a function of displacement as follows



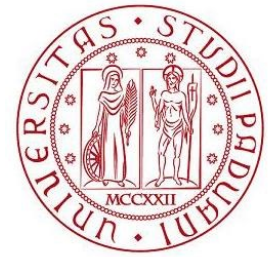
$$\delta_{cN+\Delta N} = \delta_{cN} - B (\delta_{N+\Delta N} - \delta_0)^n \Delta N$$

$\delta_{cN+\Delta N}$: Is the failure displacement of a spring after $N + \Delta N$ load cycles

B, n : Constants related to the material behaviour

The total damage:

$$D_{N+\Delta N} = \frac{\delta_0 \delta_{cN+\Delta N}}{\delta_{cN+\Delta N} - \delta_0} \left(\frac{1}{\delta_0} - \frac{1}{\delta_{N+\Delta N}} \right)$$



Third strategy

It is assumed that the fatigue damage term has an expression as

$$i \quad \frac{\partial D_f}{\partial N} = A' \left(\frac{\delta}{\delta_c} \right)^{m'}$$

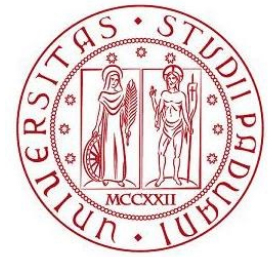
$$\int_N^{N+\Delta N} \frac{\partial D_f}{\partial N} dN \approx A' \Delta N \left(\frac{1}{2} \left(\frac{\delta_N}{\delta_c} + \frac{\delta_{N+\Delta N}}{\delta_c} \right) \right)^{m'}$$

A' and m' are constants related to the material behaviour

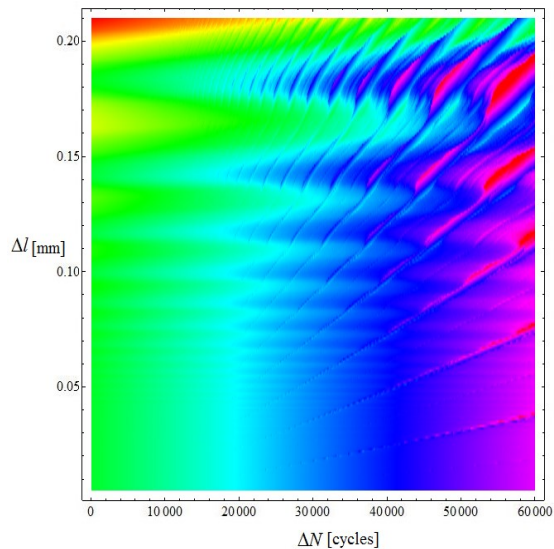
$\delta_{N+\Delta N}$: displacement of each spring after $N + \Delta N$ load cycles

The increment of total damage due to an increment of the number of cycles (ΔN) is

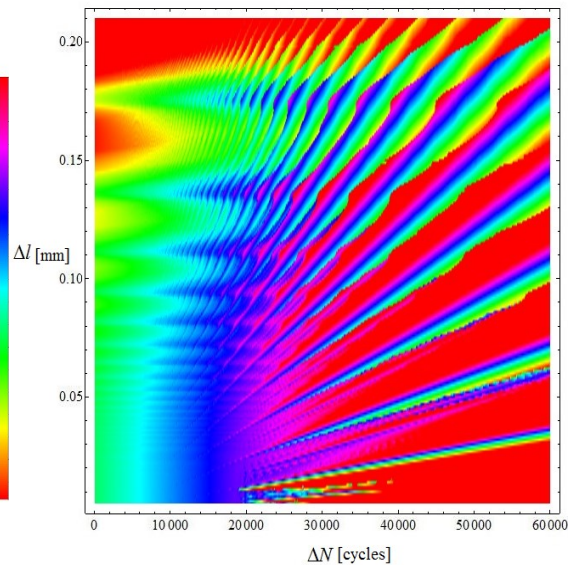
$$D_{N+\Delta N} - D_N = \underbrace{\frac{\delta_0 \delta_c}{\delta_c} \left(\frac{1}{\delta_c} - \frac{1}{\delta_c} \right)}_{\text{sum}} + \underbrace{A' \Delta N \left(\frac{1}{\delta_c} \left(\frac{\delta_N}{\delta_c} + \frac{\delta_{N+\Delta N}}{\delta_c} \right) \right)^{m'}}_{\text{jumlah}}$$



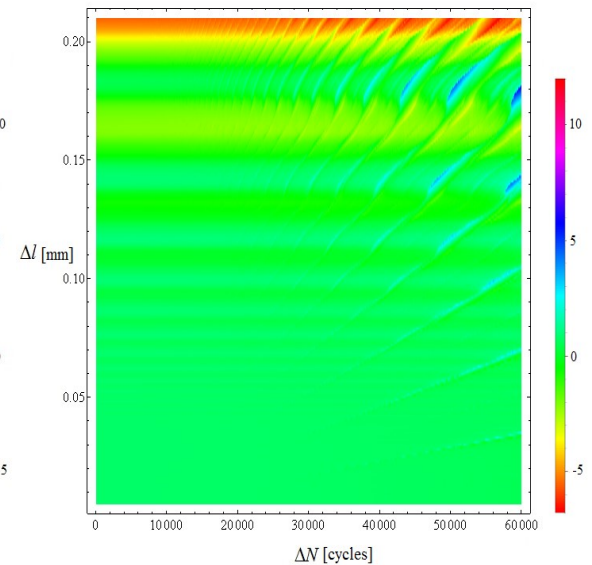
- ❑ ‘Exact slope’ (dX_{con}/dN) computed numerically using a small value of Δl ($=0.005$) and ΔN ($=100$).
- ❑ The value of the ‘exact slope’ is the same for all three formulations.



First fatigue Law

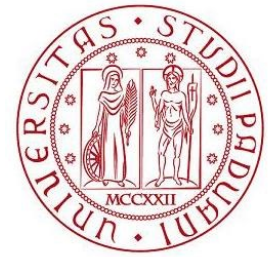


Second fatigue Law



Third fatigue Law

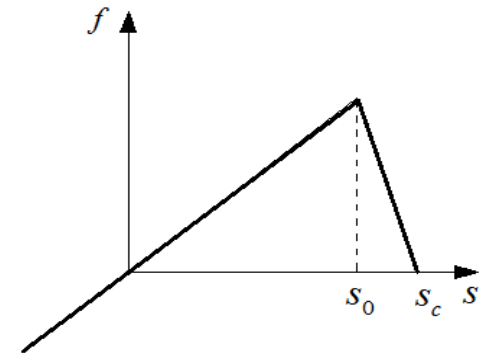
Therefore, the simple cylinder model seems to suggest that the third fatigue law is preferable



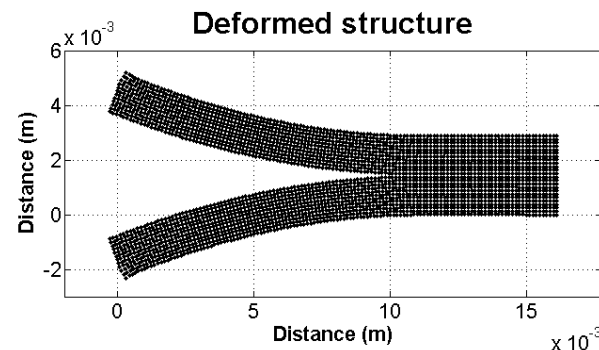
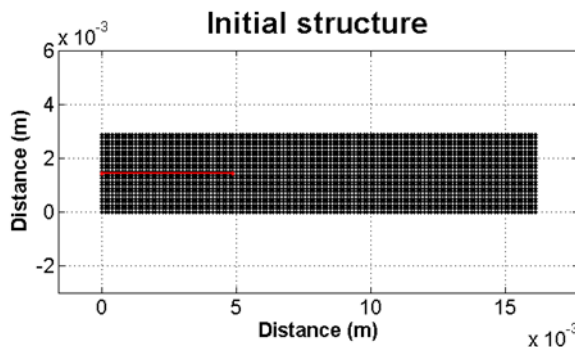
Peridynamics implementation of the fatigue model

Using a bilinear constitutive law, one may define the pairwise force function magnitude

$$\begin{cases} f(s) = c s & 0 \leq s \leq s_0 \\ f(s) = c(1-D)s & s_0 < s < s_c \\ f(s) = 0 & s \geq s_c \end{cases}$$



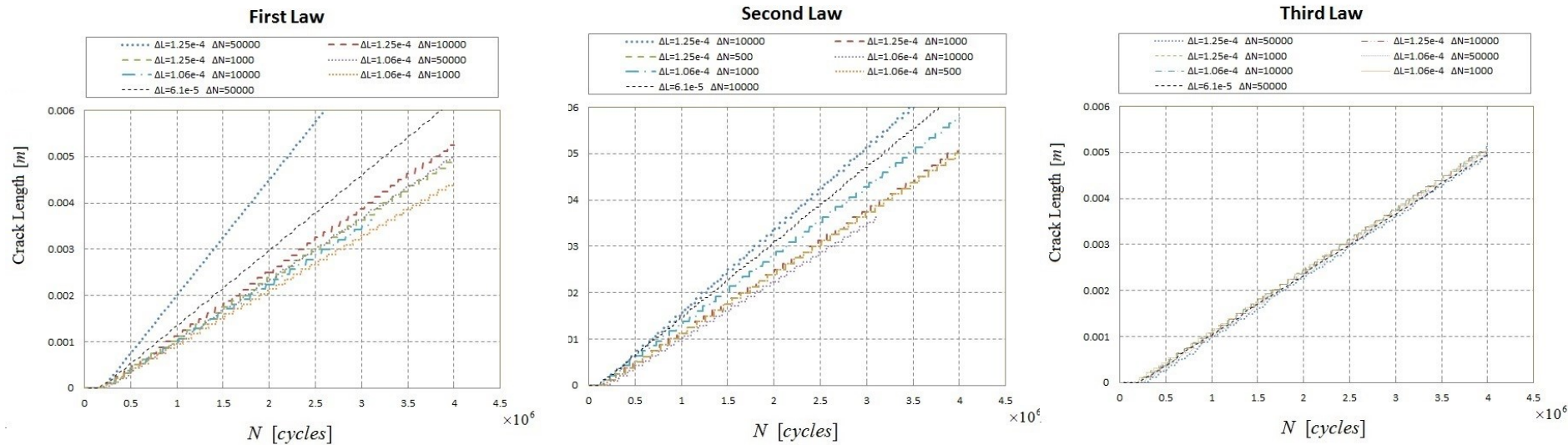
Double cantilever Beam Peridynamic Example



$$\begin{aligned} L &= 0.0161 \text{ m} & a &= 0.005 \text{ m} \\ W &= 0.0029 \text{ m} & k_r &= 20 \\ E &= 70 \text{ GPa} & M_a &= 0.048 \text{ Nm} \end{aligned}$$

$$\text{grid spacing} \left\{ \begin{array}{l} \Delta l = 6.27 \times 10^{-5} \text{ m} \\ \Delta l = 1.06 \times 10^{-4} \text{ m} \\ \Delta l = 1.25 \times 10^{-4} \text{ m} \end{array} \right. \Delta N = \left\{ \begin{array}{l} 500 \\ 1000 \\ 10000 \\ 50000 \end{array} \right.$$

In this example, the crack length with respect to the number of load cycles, N , is computed by using the three fatigue strategies



□ Both the cylinder model and the DCB discretized with the peridynamic based code confirm that the third law is the best of the three considered in the present work because it is more stable with respect to the variations of the discretization parameters and it is cheaper from a computational point of view.

□ Simulation of thermo-mechanical problems in brittle materials

- Propulsion systems of space rockets
- Nuclear fuel pallets
- Engine of the aircrafts



Some issues: Uniform discretization

In the **conventional way** of numerical implementation, the body is discretized into a **uniform grid** of points called nodes. (Approach by Silling, SA; Askari, E)

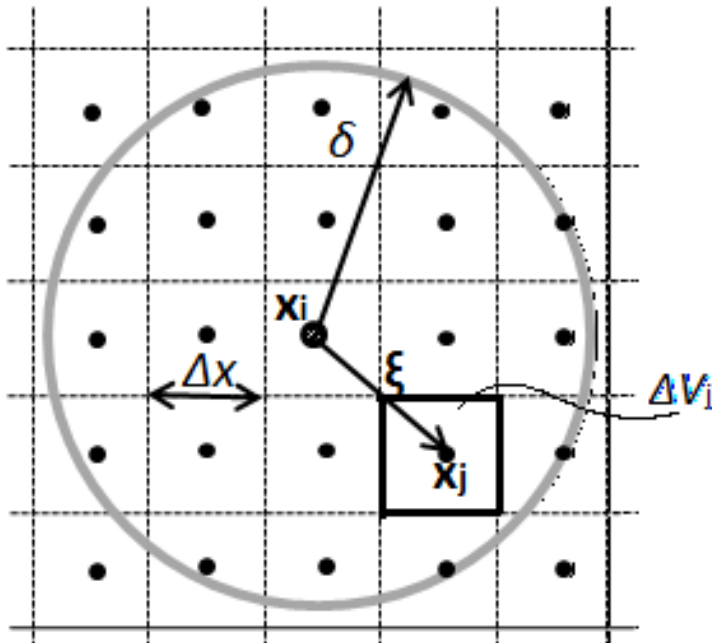
Discretized formulation in dynamic analysis

$$\rho \ddot{\mathbf{u}}_i = \left\{ \nabla_{i,j} \left\{ \underline{\mathbf{T}}[\mathbf{x}_i^n] \langle \mathbf{x}_j^n - \mathbf{x}_i^n \rangle - \underline{\mathbf{T}}[\mathbf{x}_j^n] \langle \mathbf{x}_i^n - \mathbf{x}_j^n \rangle \right\} \beta(\xi) V_j + \mathbf{b}_n^i \right. \\ \left. \left\{ \sum_j \mathbf{f}(\mathbf{u}_j^n - \mathbf{u}_i^n, \mathbf{x}_j^n - \mathbf{x}_i^n) \beta(\xi) V_j + \mathbf{b}_n^i \right\}, \forall \mathbf{x}_j \in H(\mathbf{x}_i) \right.$$

- Due to multiple nonlocal interactions, peridynamic models are most often **computationally more expensive** than classical models

- **Non-uniform** discretization (variable horizon) leads to **spurious reflection of waves** and emergence of **ghost forces**

- The whole domain must be refined when a denser grid spacing for localized areas is required; for instance, **in the case of crack propagation** and multi-scale modelling of materials

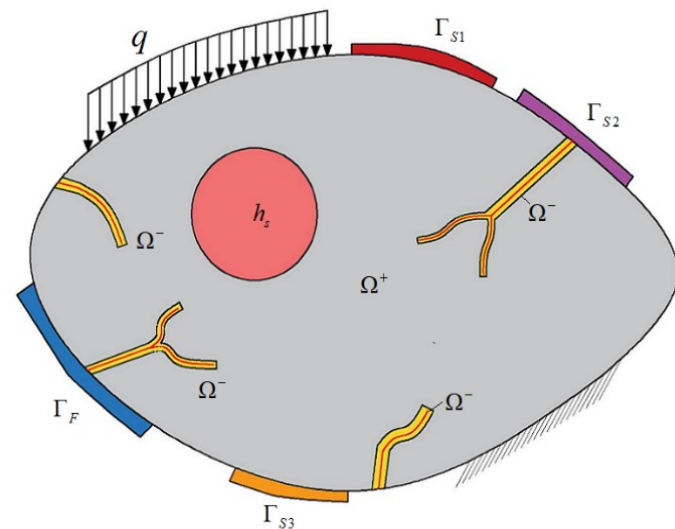
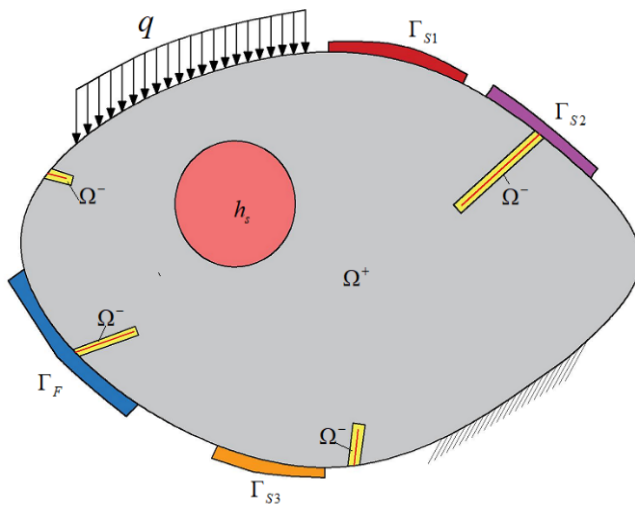


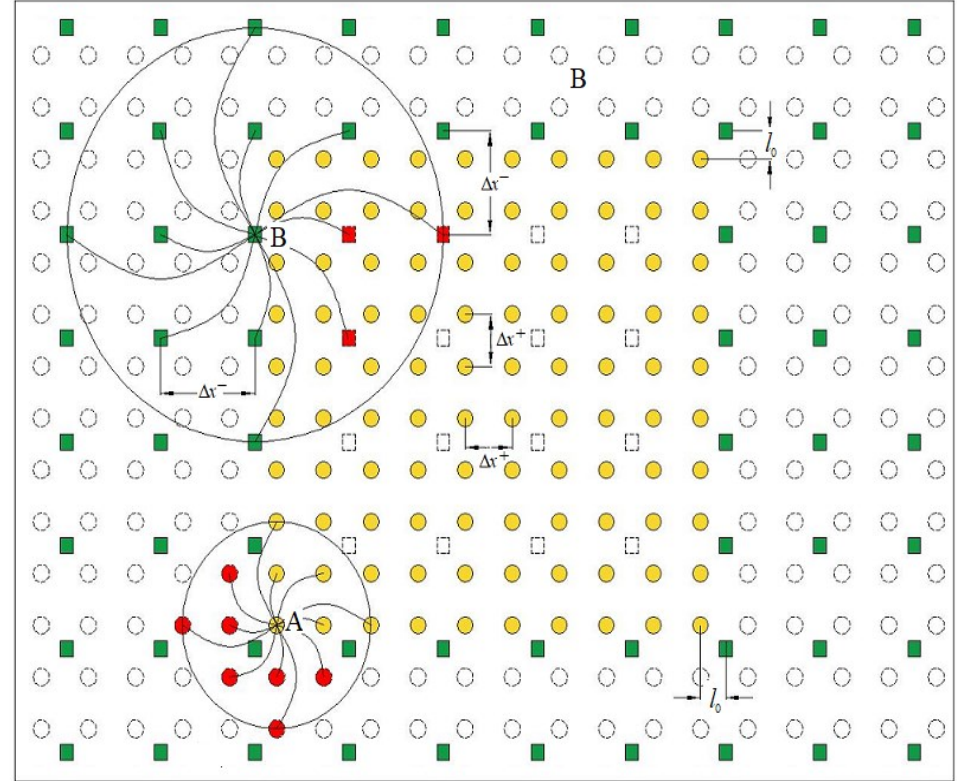
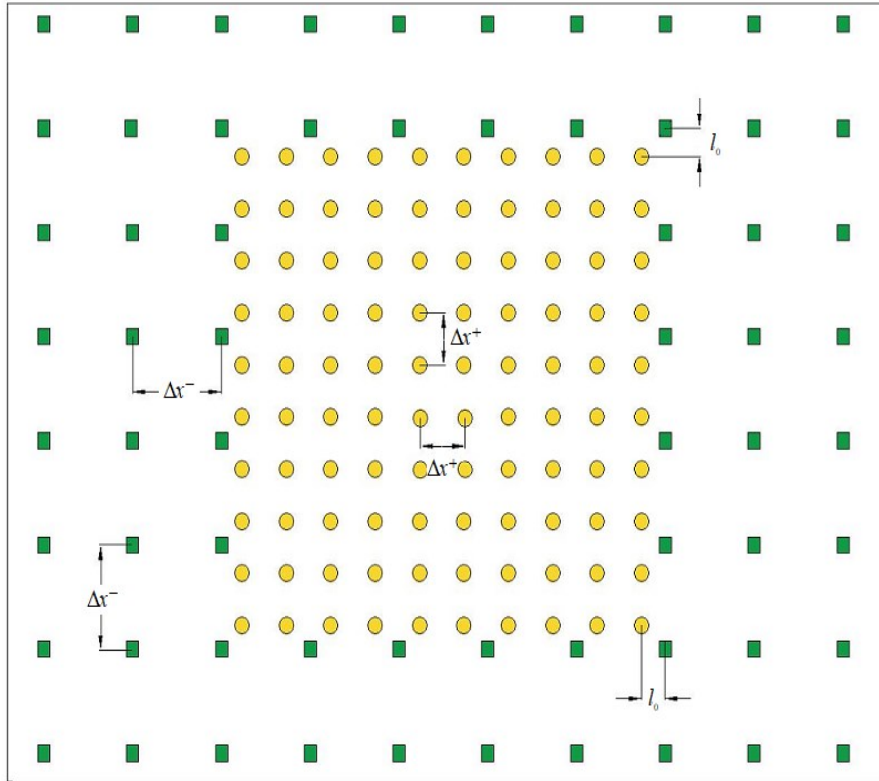
$m = \delta / \Delta x = 2.25$ in the figure

Discretization strategy

- the solution domain, Ω , is divided into two subdivisions: Ω^+ and Ω^-
- In this study, it is assumed that the finely discretized zone, Ω^- grows only where it is essential
- h_s : Heat source due to volumetric heat generation
- **Thermal boundary conditions**

Temperature (Γ_F), Heatflux (Γ_{S1}), Convection (Γ_{S2}) and radiation (Γ_{S3})

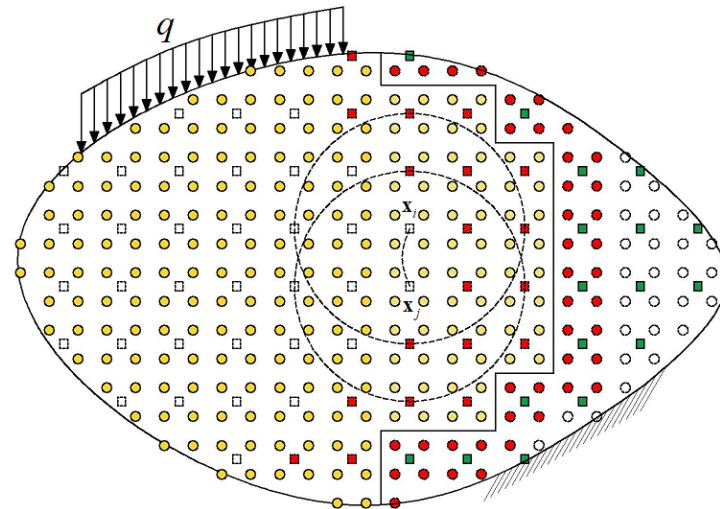
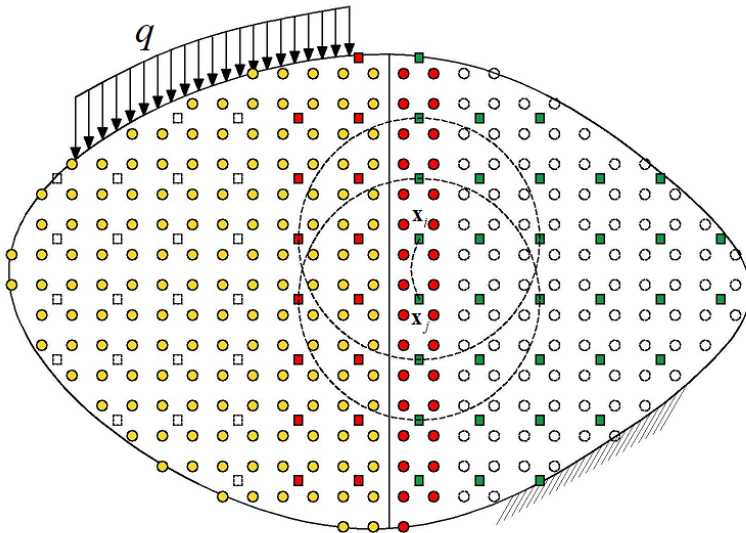


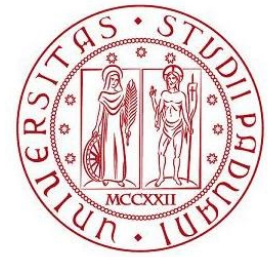


Adaptivity

$$s_{ij}^n = \frac{\|(\mathbf{x}_j + \mathbf{u}_j^n) - (\mathbf{x}_i + \mathbf{u}_i^n)\|}{\|\mathbf{x}_j - \mathbf{x}_i\|} - 1$$

$$\chi s_0 \leq s_{ij}^n - \alpha T_{avg} \leq s_0, \quad 0 < \chi < 1$$





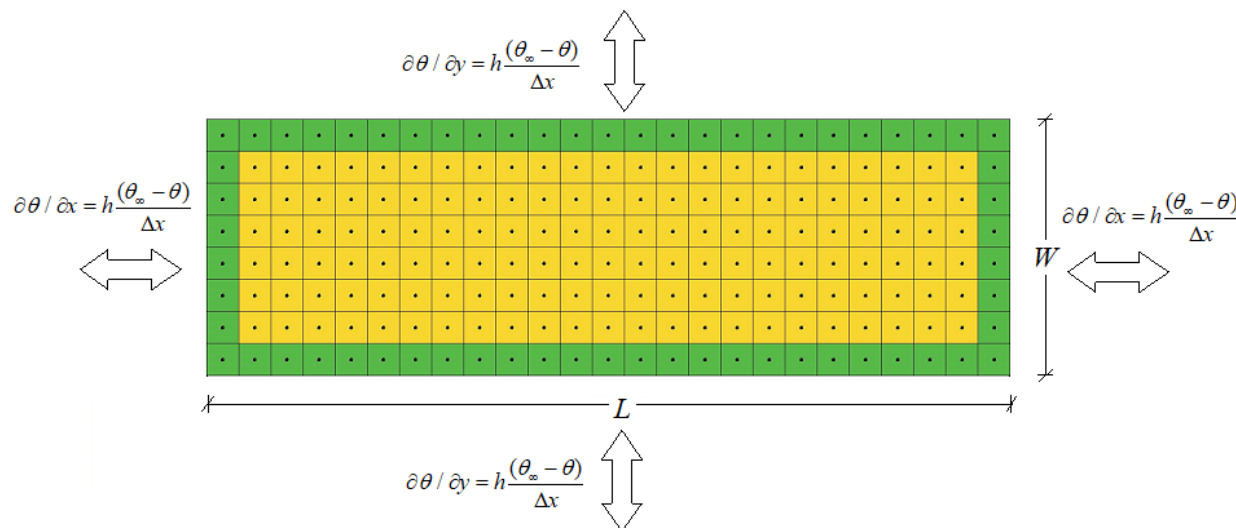
Quenching test of rectangular specimen under central thermal shock

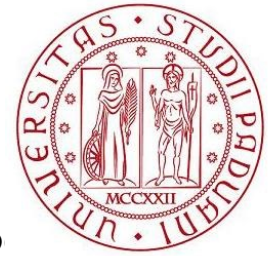
Mechanical, thermal and geometric properties of the domain under exam.

Specific heat	880 J kg ⁻¹ K ⁻¹
Thermal expansion coeff.	7.2 μK ⁻¹
Thermal conductivity	18 W m ⁻¹ K ⁻¹
Bulk modulus	227 GPa
Shear modulus	136 GPa
Density	3950 kg m ⁻³
Fracture toughness	42.27 J m ⁻²
Width X	6 cm
Depth Y	6 cm

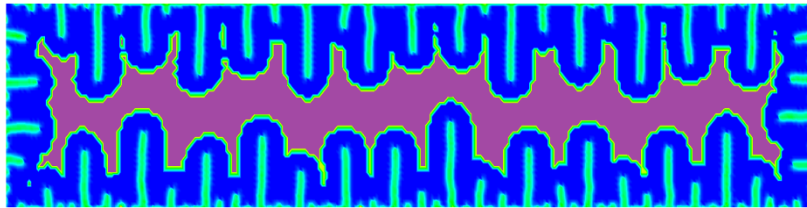
$\theta_0 = 680 \text{ K}$ → Initial temperature

$\theta_\infty = 300 \text{ K}$ → The temperature of the surfaces contacted with water



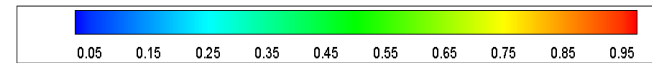


Damage in the refined model



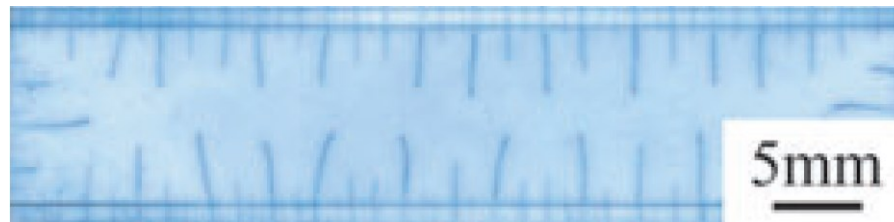
$$\Delta x^- = 0.00014 \quad \Delta x^+ = 0.00028$$

Damage in the uniform mo

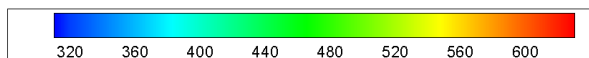
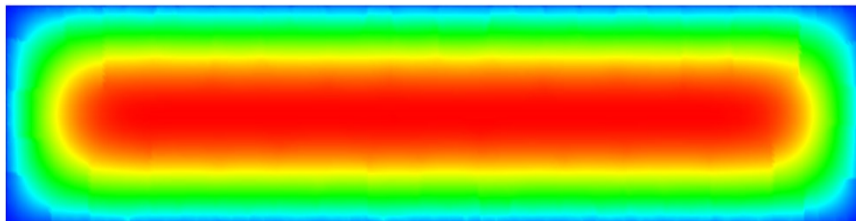


$$\Delta x = 0.00014$$

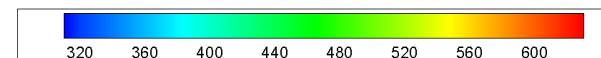
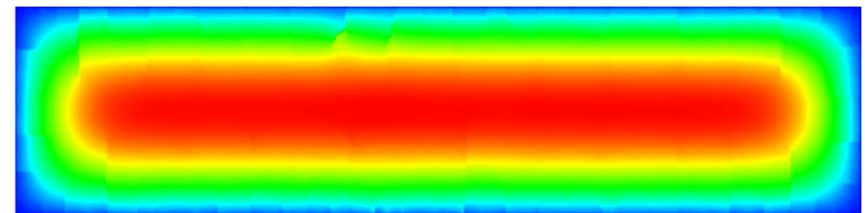
Experimental results of quenching test by (Shao et al. 2011)

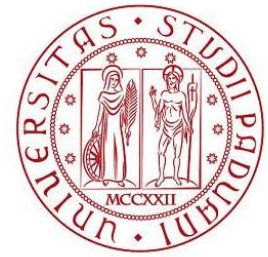


Temperature in the refined model

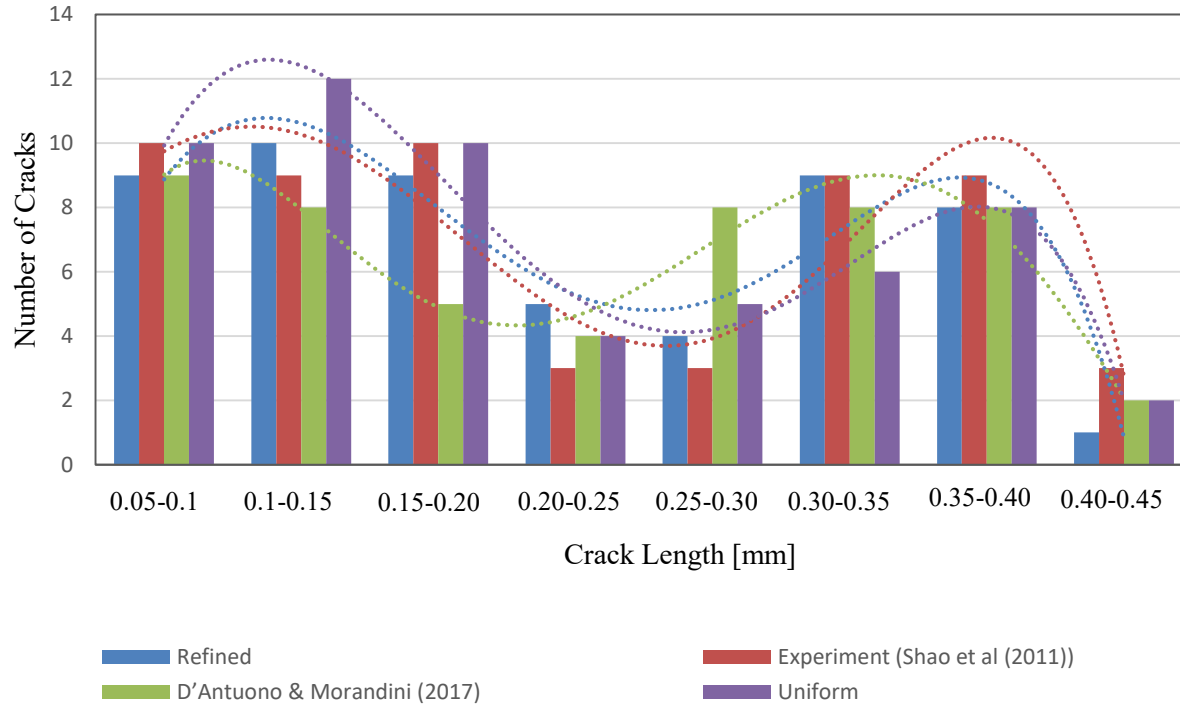


Temperature in the uniform model





Crack frequency diagram

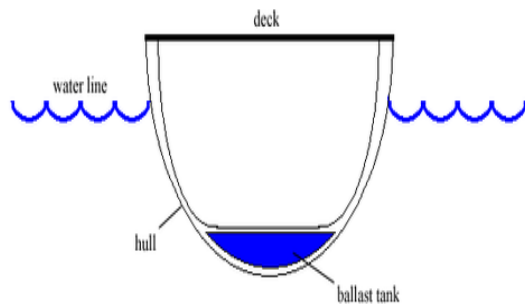
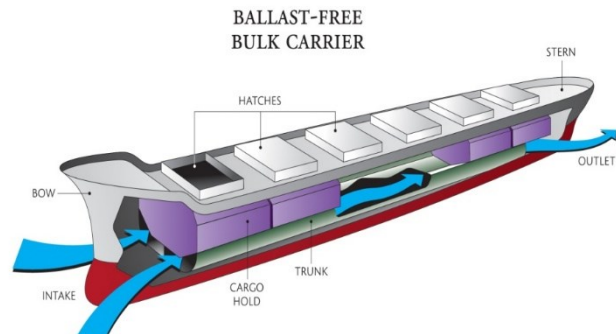


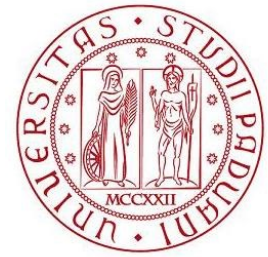
Comparison of the computational resources used by uniform and refined models

	Number of real nodes		
	Uniform	Refined	
		Coarse	Fine
$t = 0$ s	24921	3741	0
$t = 1.0$ s		1799	17000
Run time	2016.31 s	817.60 s	

Sloshing phenomena

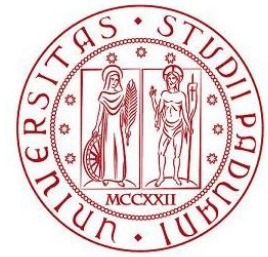
- Ocean, Maritime and coastal engineering e.g. ballast tanks of ships
- Aerospace engineering and Propulsion systems
- Tuned liquid dampers





The Peridynamic differential operator (PDDO)

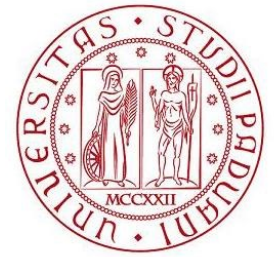
- A new mesh-free method known as PDDO has been **proposed by Madenci et al** in 2016 and 2017.
- The capability of this operator is to **construct solutions to ordinary and partial differential equations** and derivatives of scattered data e.g. velocity potential.
- Recast the numerical **differentiation up to an arbitrary order** through integration by using orthogonality properties of Peridynamic functions.
- Field equation and its **derivatives are valid everywhere** in the domain/boundaries.
- Obtain a unified solution for PDEs **without any special treatment** or **derivative reduction process**.



Applying PDDO to liquid sloshing problems

- The derivatives of the scalar field (Potential flow) play an important role in updating the **accuracy of velocities and geometry**.
- Installing baffles inside liquid tanks is also a crucial issue in liquid sloshing problems.





PDDO formulation-1

By considering the Taylor series expansion of a scalar field, $f(\mathbf{x}') = f(\mathbf{x} + \xi)$

PDDO in a two-dimensional domain, $\mathbf{x} = (x, y)$ can be constructed as

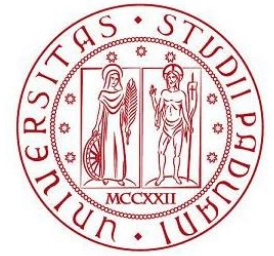
$$f(\mathbf{x} + \xi) = \sum_{n_x=0}^2 \sum_{n_y=0}^{2-n_x} \frac{1}{n_x! n_y!} \xi_x^{n_x} \xi_y^{n_y} \frac{\partial^{n_x+n_y} f(\mathbf{x})}{\partial x^{n_x} \partial y^{n_y}} + R(\mathbf{x})$$

$$n_x, n_y = 0, 1, 2$$

$$\xi = (\xi_x, \xi_y) = \mathbf{x}' - \mathbf{x}$$

If, $R(x) \rightarrow 0$, then

$$f(\mathbf{x} + \xi) = f(\mathbf{x}) + \xi_x \frac{\partial f(\mathbf{x})}{\partial x} + \xi_y \frac{\partial f(\mathbf{x})}{\partial y} + \frac{1}{2} \xi_x^2 \frac{\partial^2 f(\mathbf{x})}{\partial x^2} + \frac{1}{2} \xi_y^2 \frac{\partial^2 f(\mathbf{x})}{\partial y^2} + \xi_x \xi_y \frac{\partial^2 f(\mathbf{x})}{\partial x \partial y}$$



PDDO formulation-2

By multiplying Peridynamic functions, $g^{p_x p_y}(\xi)$, which possess an orthogonality property, and then integrating them over the horizon of each node

$$\int_{H_x} f(\mathbf{x} + \xi) g^{p_x p_y}(\xi) dV = f(\mathbf{x}) \int_{H_x} g^{p_x p_y}(\xi) dV + \frac{\partial f(\mathbf{x})}{\partial x} \int_{H_x} \xi_x g^{p_x p_y}(\xi) dV + \frac{\partial f(\mathbf{x})}{\partial y} \int_{H_x} \xi_y g^{p_x p_y}(\xi) dV + \frac{\partial^2 f(\mathbf{x})}{\partial x^2} \int_{H_x} \frac{1}{2} \xi_x^2 g^{p_x p_y}(\xi) dV + \frac{\partial^2 f(\mathbf{x})}{\partial y^2} \int_{H_x} \frac{1}{2} \xi_y^2 g^{p_x p_y}(\xi) dV + \frac{\partial^2 f(\mathbf{x})}{\partial x \partial y} \int_{H_x} \xi_x \xi_y g^{p_x p_y}(\xi) dV$$

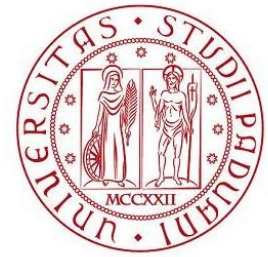
Since Peridynamic functions, $g^{p_x p_y}$, possess an orthogonality property

$$\frac{1}{n_x! n_y!} \int_{H_x} \xi_x^{n_x} \xi_y^{n_y} g^{p_x p_y}(\xi) dV = \delta_{n_x p_x} \delta_{n_y p_y}$$

$$g^{p_x p_y}(\xi) = \sum_{q_x=0}^2 \sum_{q_y=0}^{2-q_x} a_{q_x}^{p_x} a_{q_y}^{p_y} w_{q_x q_y}(\|\xi\|) \xi_x^{q_x} \xi_y^{q_y}$$

The weight function is constructed based on a Gaussian distribution as follows

$$w(\|\xi\|) = e^{-(2\|\xi\|/\delta)^2}$$

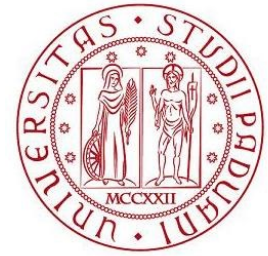


PDDO formulation

By considering the Taylor series expansion of a scalar field, $f(\mathbf{x}') = f(\mathbf{x} + \xi)$

one can compute derivatives explicitly:

$$\begin{array}{ccc}
 \text{2D} & & \text{3D} \\
 \left\{ \begin{array}{l} f(\mathbf{x}) \\ \frac{\partial f(\mathbf{x})}{\partial x} \\ \frac{\partial f(\mathbf{x})}{\partial y} \\ \frac{\partial^2 f(\mathbf{x})}{\partial x^2} \\ \frac{\partial^2 f(\mathbf{x})}{\partial y^2} \\ \frac{\partial^2 f(\mathbf{x})}{\partial x \partial y} \end{array} \right\} = \int_{H_x} f(\mathbf{x} + \xi) \left\{ \begin{array}{l} g^{00}(\xi) \\ g^{10}(\xi) \\ g^{01}(\xi) \\ g^{20}(\xi) \\ g^{02}(\xi) \\ g^{11}(\xi) \end{array} \right\} dV & \xrightarrow{\text{Likewise}} & \left\{ \begin{array}{l} f(\mathbf{x}) \\ \frac{\partial f(\mathbf{x})}{\partial x} \\ \frac{\partial f(\mathbf{x})}{\partial y} \\ \frac{\partial f(\mathbf{x})}{\partial z} \\ \frac{\partial^2 f(\mathbf{x})}{\partial x^2} \\ \frac{\partial^2 f(\mathbf{x})}{\partial y^2} \\ \frac{\partial^2 f(\mathbf{x})}{\partial z^2} \\ \frac{\partial^2 f(\mathbf{x})}{\partial x \partial y} \\ \frac{\partial^2 f(\mathbf{x})}{\partial x \partial z} \\ \frac{\partial^2 f(\mathbf{x})}{\partial y \partial z} \end{array} \right\} = \int_{H_x} f(\mathbf{x} + \xi) \left\{ \begin{array}{l} g^{000}(\xi) \\ g^{100}(\xi) \\ g^{010}(\xi) \\ g^{001}(\xi) \\ g^{200}(\xi) \\ g^{020}(\xi) \\ g^{002}(\xi) \\ g^{110}(\xi) \\ g^{101}(\xi) \\ g^{011}(\xi) \end{array} \right\} dV
 \end{array}$$



Governing Lagrangian equations

- For an **irrotational flow**, potential flow theory can be used:

$$\mathbf{u} = \nabla \varphi$$

- For an **incompressible fluid**:

$$\nabla \cdot \mathbf{u} = 0$$

- Consequently, **velocity potential**, has to satisfy the Laplace equation:

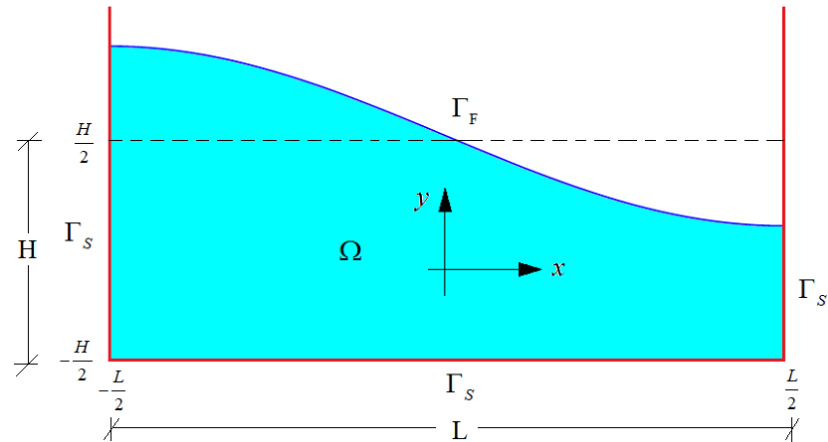
$$\nabla^2 \varphi = 0 \quad \text{in } \Omega$$

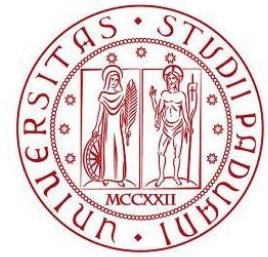
Boundary conditions

$$\frac{\partial \varphi}{\partial n} = \mathbf{n}^T \mathbf{u} \quad \text{On } \Gamma_s$$

Dynamic free surface boundary conditions (DFSBC)

$$\frac{d\varphi}{dt} = g\left(y + \frac{H}{2}\right) + \frac{1}{2}(\nabla \varphi \cdot \nabla \varphi) \quad \text{On } \Gamma_F$$





- Non-linear liquid sloshing under harmonic excitation**

$$g=9.81 \text{ m/s}^2, \rho=1000 \text{ kg/m}^3$$

Periodic sinusoidal excitation:

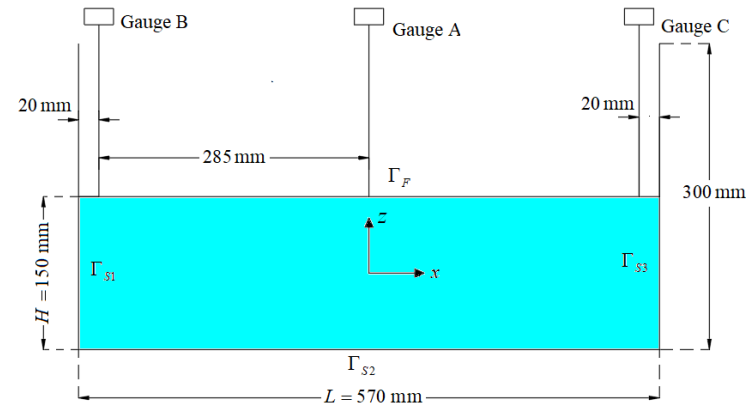
$$x_T = -A \sin \omega t$$

$$\Delta t = 0.01 \text{ s}, \quad \omega = 1.0 \omega_0, \quad A = 0.005 \text{ m}$$

$\omega_0 \rightarrow$ natural frequency of tank

Grid (PDDO): 12×5 Grid (VOF): 114×64

The boundary condition values in terms of PD unknowns

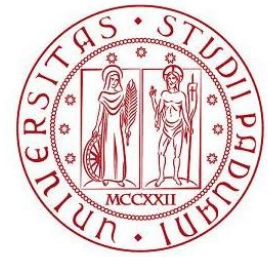


$$\sum_{j=1} \varphi(x_j, z_j) g^{01}(\mathbf{x}_j - \mathbf{x}_i, \mathbf{z}_j - \mathbf{z}_i) \mathbf{V}_j = 0 \quad \text{for } z_i = -\frac{H}{2}$$

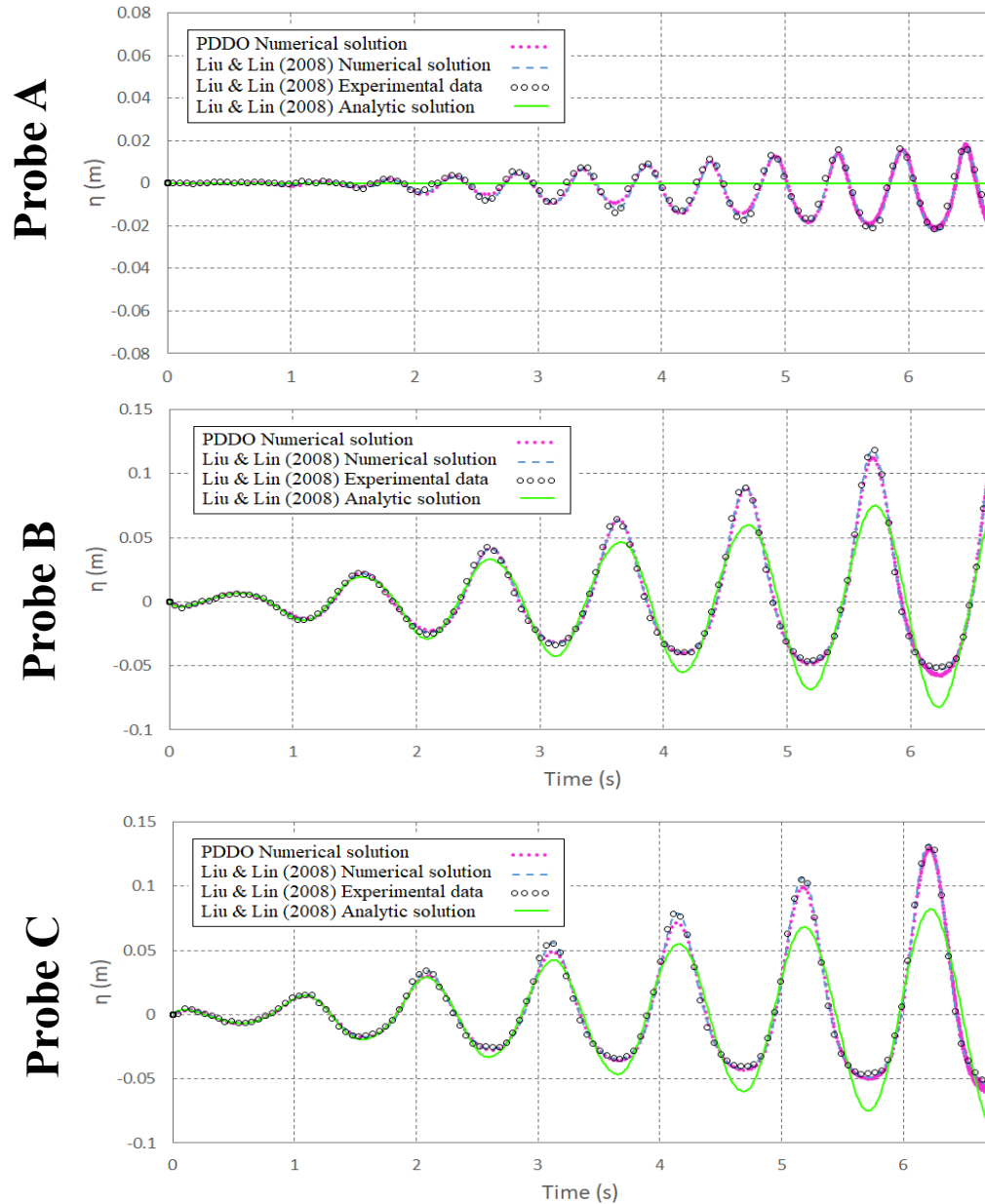
$$\sum_{j=1} \varphi(x_j, z_j) g^{10}(\mathbf{x}_j - \mathbf{x}_i, \mathbf{z}_j - \mathbf{z}_i) \mathbf{V}_j = A \omega \sin \omega t \quad \text{for } x_i = -\frac{L}{2}$$

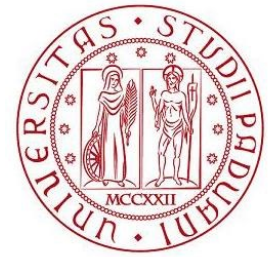
$$\sum_{j=1} \varphi(x_j, z_j) g^{10}(\mathbf{x}_j - \mathbf{x}_i, \mathbf{z}_j - \mathbf{z}_i) \mathbf{V}_j = -A \omega \sin \omega t \quad \text{for } x_i = \frac{L}{2}$$

$$\sum_{j=1} \varphi(x_j, z_j) g^{00}(\mathbf{x}_j - \mathbf{x}_i, \mathbf{z}_j - \mathbf{z}_i) \mathbf{V}_j = (\varphi_i)^{(n-2)} + 2 \Delta t \left[\left(-g \left(z + \frac{H}{2} \right) + \frac{1}{2} \nabla \varphi \cdot \nabla \varphi \right)_i \right]^{(n-1)} \quad \text{for } (x_i, z_i) \in \Gamma_F$$



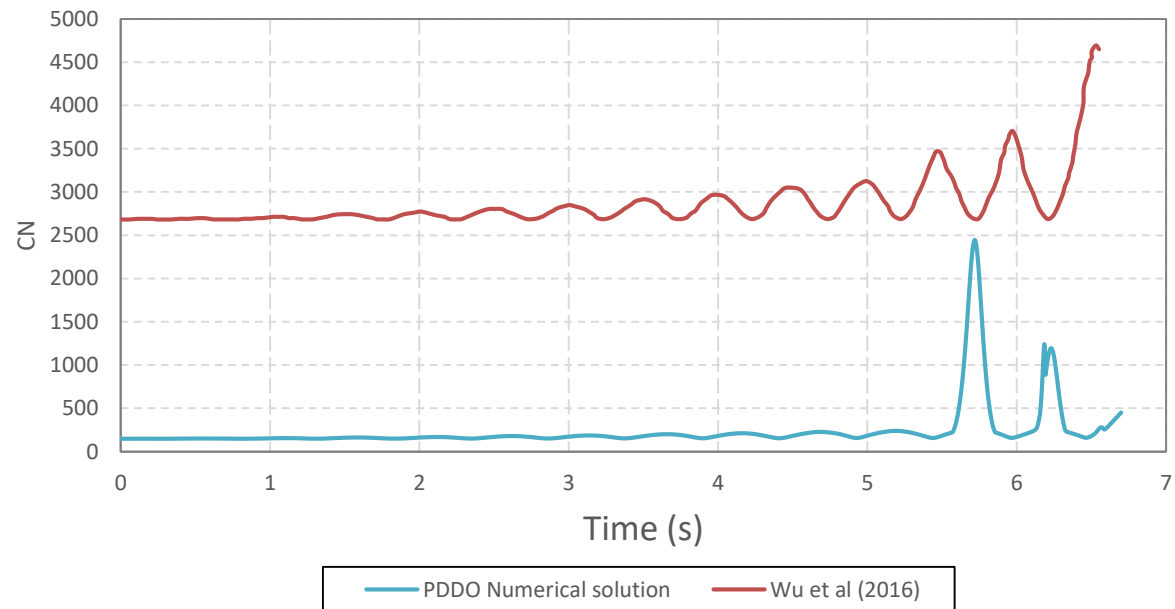
Comparisons of the time series of surface elevation



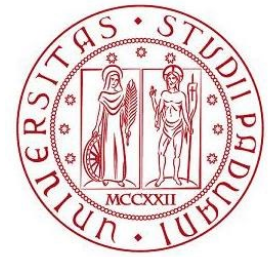


The Condition Number (CN) of the global stiffness matrix

$$CN = \|\mathbf{k}\|_2 \|\mathbf{k}^{-1}\|_2$$



- The histogram of the global stiffness matrix for non-linear liquid sloshing under lateral excitation.
- PDDO generates a **well-conditioned sparse system of equations** in time in comparison with **local polynomial collocation method**.



- 2D liquid sloshing in a tank with a vertical baffle**

$L = 1.0 \text{ m}$

$H = 0.5 \text{ m}$

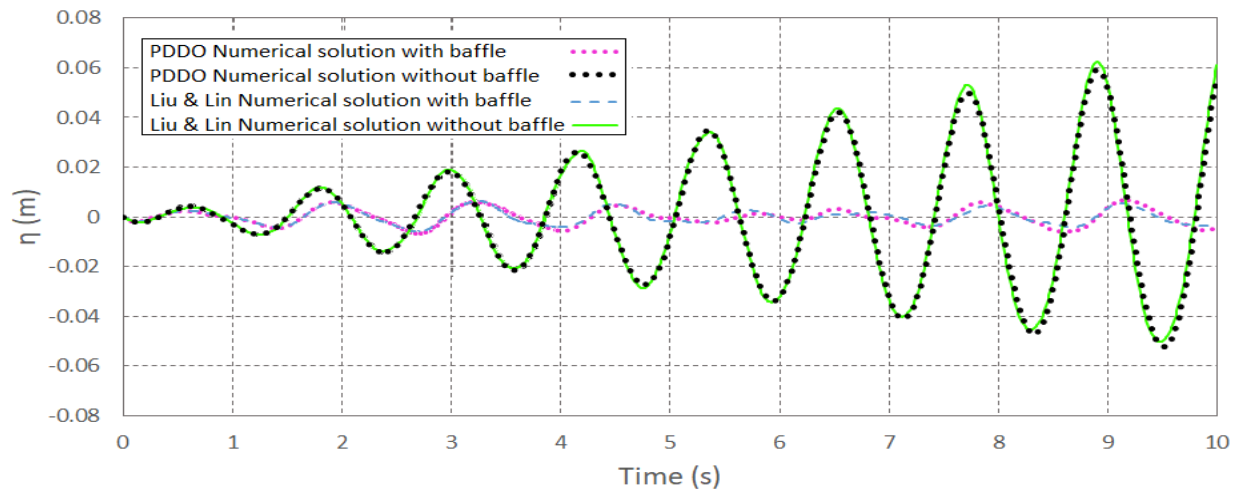
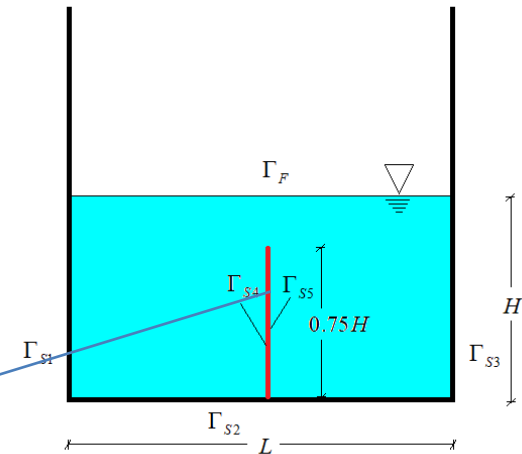
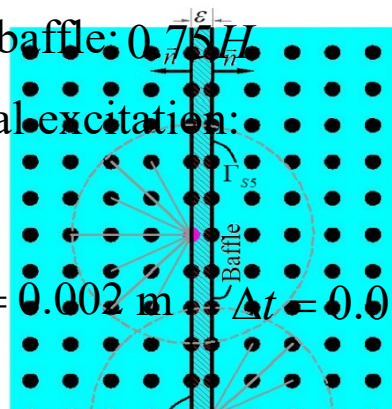
The height of the baffle: $0.75H$

Periodic sinusoidal excitation:

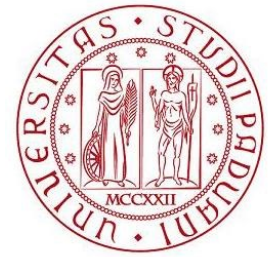
$x_T = -A \sin \omega t$

$\omega = 5.29 \text{ rad/s}$ $A = 0.002 \text{ m}$ $\Delta t = 0.01 \text{ s}$

Grid: 51×26



Comparisons of the time series of surface elevation η at the right boundary of the tank.



- **3D nonlinear liquid sloshing under periodic excitations in a square tank**

$$L = B = 1.0 \text{ m}$$

$$H = 0.5 \text{ m}$$

$$\varphi = 30^\circ$$

$$\omega_0 = 4.4957 \text{ rad/s}$$

Periodic excitation:

$$u_x = -A\omega \cos(\varphi) \sin(\omega t), \quad u_y = -A\omega \sin(\varphi) \cos(\omega t)$$

$$\omega = 0.9\omega_0 \quad A = 0.005 \text{ m} \quad \Delta t = 0.01 \text{ s}$$

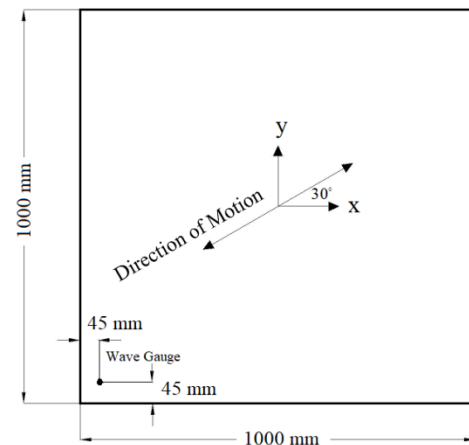
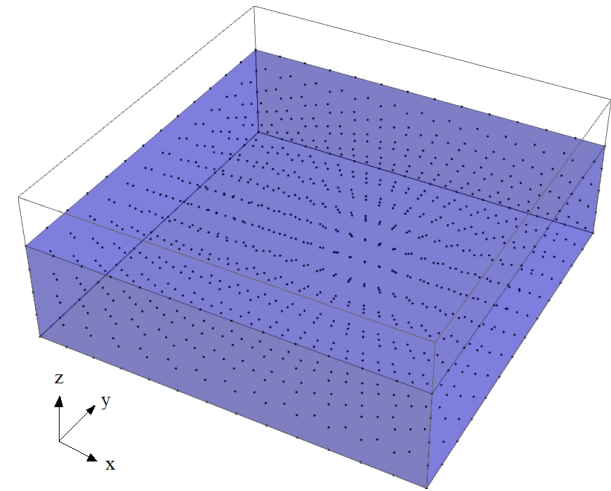
Grid: $14 \times 14 \times 5$

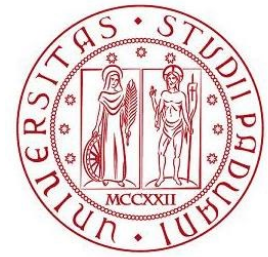
PDDO:

980 nodes are employed.

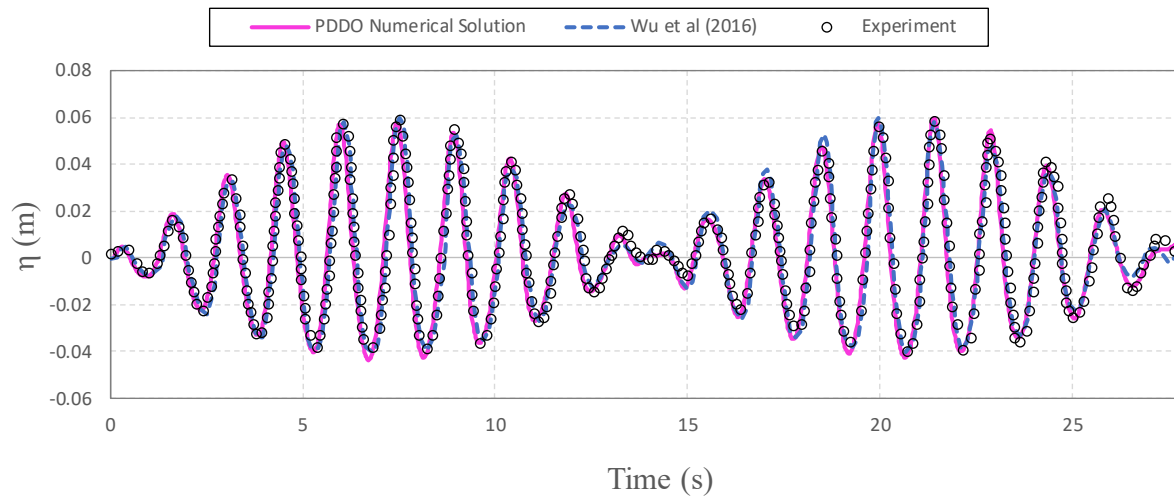
Local polynomial collocation method:

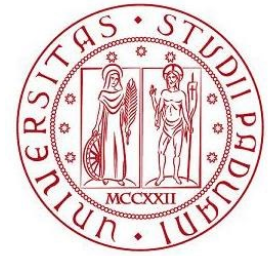
1005 nodes are employed.





Comparison of the surface elevations obtained by the present method, polynomial collocation method and the experimental data at the corner of the tank .





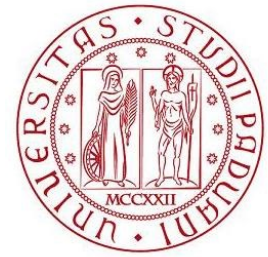
Conclusions

➤ Fatigue crack propagation in structural components

- ❑ We compare three fatigue degradation strategies to be used in the simulation of fatigue crack propagation.
- ❑ The third fatigue degradation strategy is the best, among those investigated, for being used in BBPD codes.
- ❑ The cylinder model appears to provide reliable indications about the computational performance of the fatigue laws.

➤ Crack phenomena due to thermal shocks

- ❑ This study presents an effective way to use a variable grid size in weakly coupled thermal shock peridynamic model.
- ❑ The refinement numerical method is equipped with stretch control criterion to transform the grid discretization adaptively in time. Hence, finer grid spacing is only applied in limited zones where it is required.



Conclusions

➤ Crack phenomena due to thermal shocks

- ❑ The results confirm that the method is capable of producing the results of a standard peridynamic model with uniform discretization at a much **smaller computational cost**.

➤ Sloshing of fluids in tanks.

- ❑ PDDO is capable to produce a **well-conditioned system of equations** for the problem which is important for marching in time.
- ❑ 2D and 3D challenging liquid sloshing **problems with strong non linearity** have been solved and the results are compared with other numerical/analytical/experimental results in literature.
- ❑ To further validate the method, we investigate liquid sloshing in rectangular **tanks containing vertical baffles**.
- ❑ The newly proposed method (PDDO) is unique in its combination of **high accuracy, high stability and low computational cost**.

**Thanks for Your
Attention**